

# Towards the Numerical Simulation of Electrocardiograms

Muriel Boulakia<sup>2</sup>, Miguel A. Fernández<sup>1</sup>, Jean-Frédéric Gerbeau<sup>1</sup>,  
and Nejib Zenzemi<sup>1</sup>

<sup>1</sup> REO team, INRIA Rocquencourt, France

<http://www-rocq.inria.fr/REO>

<sup>2</sup> REO team, Laboratoire Jacques-Louis Lions, Université Paris 6, France

**Abstract.** We present preliminary results of the numerical simulation of electrocardiograms (ECG). We consider the bidomain equations to model the electrical activity of the heart and a Laplace equation for the torso. The ionic activity is modeled with a Mitchell-Schaeffer dynamics. We use adaptive semi-implicit BDF schemes for the time discretization and a Neumann-Robin domain decomposition algorithm for the space discretization. The obtained ECGs, although not completely satisfactory, are promising. They allow to discuss various modelling assumptions, for example the relevance of cells heterogeneity, the fiber orientation and the coupling conditions with the torso.

## 1 Introduction

We address the numerical simulation of electrocardiograms (ECG), namely the direct problem of cardiac electrophysiology. Our basic equations are the so-called bidomain model for the heart [4,16] coupled to a simple model for the torso.

The complexity of the electrical activity of the heart raise many modelling issues: strong nonlinearity due to the ionic currents, stiffness due to very different time scales, heterogeneity of cells, anisotropy due to the fibers, *etc.* Moreover, the modelling of many aspects of the problem is not yet well-established. In [20], more than 28 models of cardiac cells are reported, some of them including more than 50 parameters. The coupling conditions between the heart and the torso are also subject to controversy [11].

We have to face two opposite viewpoints: on the one hand, we would like to model as accurately as possible the physical phenomena described in the literature; on the other hand, we would like to keep as low as possible the complexity of the model, both in terms of computational effort and in terms of number of parameters. Our purpose is to obtain ECGs, and we propose to address, with the help of numerical simulations, what could be the “minimum requirements” of the model to reach this goal. For example, is a bidomain model necessary? what is the effect of the heart movement? how sensitive are the results to the anisotropy induced by fibers or the cells heterogeneity? is it really useful to strongly couple the heart with the torso? what should be the coupling conditions? how to handle the His bundle and the Purkinje fibers? *etc.* We do not address all these

questions in this paper. The point is mainly to present preliminary results and to draw some perspectives.

## 2 Modelling

We denote by  $\Omega_H$  the total domain occupied by the heart. In the microscopic scale, the cardiac tissue is assumed to be composed of two distinct media: the intracellular media, made of the cardiac cells, and the extracellular media, composed of the remainder of the heart. After an homogenization process, the intra- and extracellular domains are superimposed and occupy the whole domain  $\Omega_H$  [16,4]. We denote by  $\mathbf{j}_i$ ,  $\mathbf{j}_e$  and  $u_i$ ,  $u_e$  the intra- and extracellular densities of current and electric potentials respectively. The homogenized equation associated to the electrical charge conservation is:

$$\operatorname{div}(\mathbf{j}_i + \mathbf{j}_e) = 0, \quad \text{in } \Omega_H. \quad (2.1)$$

The homogenized equation governing the electrical activity of the cell membranes is given by

$$A_m \left( C_m \frac{\partial V_m}{\partial t} + I_{\text{ion}}(V_m, w) \right) + \operatorname{div}(\mathbf{j}_i) = A_m I_{\text{app}}, \quad \text{in } \Omega_H, \quad (2.2)$$

where  $A_m$  is a constant representing the average rate of membrane surface per unit of volume, the function  $I_{\text{ion}}$  represents the current due to the ionic exchanges,  $I_{\text{app}}$  is a given stimulation current,  $C_m$  is a capacity per unit of area of the membrane,  $V_m$  is the transmembrane potential defined by

$$V_m = u_i - u_e, \quad (2.3)$$

and the vector function  $w$  is solution to a system of ordinary differential equations:

$$\frac{\partial w}{\partial t} + g(V_m, w) = 0. \quad (2.4)$$

The precise definition of  $g$  and  $I_{\text{ion}}$  depends on the cell model. We can use a physiological ionic model (*e.g.* [13] or [6]) or a phenomenological one (*e.g.* [7] or [15]). In this paper, we consider the phenomenological model proposed by Mitchell and Schaeffer [15]:

$$I_{\text{ion}}(V_m, w) = -\frac{w}{\tau_{in}} V_m^2 (1 - V_m) + \frac{V_m}{\tau_{out}}, \quad (2.5)$$

$$g(V_m, w) = \begin{cases} \frac{w-1}{\tau_{open}} & \text{if } V_m < V_{gate}, \\ \frac{w}{\tau_{close}} & \text{if } V_m > V_{gate}, \end{cases} \quad (2.6)$$

where  $\tau_{in}$ ,  $\tau_{out}$ ,  $\tau_{open}$ ,  $\tau_{close}$  and  $V_{gate}$  are given parameters. Note that this model is close to the model proposed in [24].

The current densities are linked to the electric potentials through the Ohm's law  $\mathbf{j}_i = -\boldsymbol{\sigma}_i \nabla u_i$ ,  $\mathbf{j}_e = -\boldsymbol{\sigma}_e \nabla u_e$ , where  $\boldsymbol{\sigma}_i$  and  $\boldsymbol{\sigma}_e$  are the intra- and extracellular conductivity tensors. The system of equations within the heart therefore reads [12,17,18]:

$$\begin{cases} A_m \left( C_m \frac{\partial V_m}{\partial t} + I_{\text{ion}}(V_m, w) \right) - \text{div}(\boldsymbol{\sigma}_i \nabla u_i) = A_m I_{\text{app}}, & \text{in } \Omega_H, \\ \text{div}(\boldsymbol{\sigma}_e \nabla u_e) = -\text{div}(\boldsymbol{\sigma}_i \nabla u_i), & \text{in } \Omega_H, \\ \partial_t w + g(V_m, w) = 0, & \text{in } \Omega_H. \end{cases} \quad (2.7)$$

This model is often studied when the heart is isolated (*cf.* for example [2,3,4]). We are interested in coupling it with a simplified model of the electrical activity of the surrounding tissues (as done for example in [5,18] or [23]). The boundary  $\partial\Omega_H$  of the domain  $\Omega_H$ , *i.e.* the interface between the heart and the extracardiac region is divided into two parts: the endocardium  $\Gamma_{\text{endo}}$  and the epicardium  $\Gamma_{\text{epi}}$ . It is generally admitted (*cf.* [17,23]) that the intracellular current  $\mathbf{j}_i$  does not propagate outside the heart. Consequently, on the heart boundary  $\Gamma_{\text{epi}} \cup \Gamma_{\text{endo}}$  we impose  $\boldsymbol{\sigma}_i \nabla u_i \cdot \mathbf{n} = 0$ . The torso domain is denoted by  $\Omega_T$  and the potential in  $\Omega_T$  by  $u_T$ . The torso is seen as a passive conductor, thus  $u_T$  satisfies a Laplace equation:

$$\text{div}(\boldsymbol{\sigma}_T \nabla u_T) = 0, \quad \text{in } \Omega_T, \quad (2.8)$$

where  $\boldsymbol{\sigma}_T$  represents the conductivity tensor of the torso. The boundary of the torso is divided into two parts: one internal  $\Gamma_{\text{epi}}$ , in contact with the heart, and  $\Gamma_{\text{ext}}$  representing the external surface of the torso. The boundary  $\Gamma_{\text{ext}}$  is supposed to be insulated, thus we impose  $\boldsymbol{\sigma}_T \nabla u_T \cdot \mathbf{n}_T = 0$  where  $\mathbf{n}_T$  is the outward unit normal on  $\Gamma_{\text{ext}}$ .

On  $\Gamma_{\text{epi}}$ , the following conditions are generally adopted in the literature:

$$\begin{cases} u_e = u_T, & \text{on } \Gamma_{\text{epi}}, \\ \boldsymbol{\sigma}_e \nabla u_e \cdot \mathbf{n} = \boldsymbol{\sigma}_T \nabla u_T \cdot \mathbf{n}, & \text{on } \Gamma_{\text{epi}}. \end{cases} \quad (2.9)$$

They are formally obtained in [11] by an homogenization procedure. They correspond to a perfect electrical coupling between the heart and the torso. Nevertheless, the heart is separated from the torso by the pericardium which is a double-walled sac containing a serous fluid. Thus, it seems reasonable to assume the more general coupling conditions:

$$\begin{cases} R_p \boldsymbol{\sigma}_e \nabla u_e \cdot \mathbf{n} = R_p C_p \frac{\partial(u_T - u_e)}{\partial t} + (u_T - u_e), & \text{on } \Gamma_{\text{epi}}, \\ \boldsymbol{\sigma}_e \nabla u_e \cdot \mathbf{n} = \boldsymbol{\sigma}_T \nabla u_T \cdot \mathbf{n}, & \text{on } \Gamma_{\text{epi}}, \end{cases} \quad (2.10)$$

which takes into account a possible capacitive ( $C_p$ ) and resistive ( $R_p$ ) effect of the pericardium. To the best of our knowledge, this effect is not documented in the literature. The influence of  $R_p$  and  $C_p$  will be investigated through numerical simulations in a forthcoming work. Of course the classical relations (2.9) can be recovered from (2.10) by setting  $R_p = 0$ .

### 3 Numerical Methods

We define the open set  $\Omega$  as the interior of  $\overline{\Omega_H} \cup \overline{\Omega_T}$ . Eliminating the unknown  $u_i$  in the previous system using (2.3), the above problem is equivalent to finding  $u_e$ ,  $u_T$ ,  $V_m$  and  $w$  such that (2.10)<sub>1</sub> and (2.4) are satisfied, and

$$A_m \int_{\Omega_H} \left( C_m \frac{\partial V_m}{\partial t} + I_{\text{ion}}(V_m, w) \right) \phi + \int_{\Omega_H} \sigma_i \nabla(V_m + u_e) \cdot \nabla \phi = \int_{\Omega_H} I_{\text{app}} \phi, \quad (3.11)$$

$$\int_{\Omega_H} (\sigma_i + \sigma_e) \nabla u_e \cdot \nabla \phi + \int_{\Omega_H} \sigma_i \nabla V_m \cdot \nabla \phi + \int_{\Omega_T} \sigma_T \nabla u_T \cdot \nabla \phi = 0, \quad (3.12)$$

for all  $\phi \in H^1(\Omega)$ . Note that this variational formulation takes into account very conveniently the coupling condition (2.10)<sub>2</sub>. Under technical assumptions on the functions  $I_{\text{ion}}$  and  $g$ , and for  $R_p = 0$ , we have proved in [1] that this system admits a unique solution. This system is discretized in space using the Lagrangian P1 finite elements and in time using a semi-implicit scheme based on the BDF (*Backward Differentiation Formula*) methods. The heart and torso domains are solved iteratively with a Neumann/Robin domain decomposition method. We denote by  $\Delta t$  the time step and we assume that the solution is known until time  $t^n$ . Here is the procedure used to compute  $(V_m^{n+1}, u_e^{n+1}, u_T^{n+1}, w^{n+1})$ .

The first step is to solve the ionic current, namely the equation (2.4) which is usually very stiff. We chose to use the `cvode` solver<sup>1</sup> which uses adaptivity, both in time and in order, and solves the implicit part of the equations with a Newton algorithm. For practical reason, it is convenient to uncouple this step from the solution of the bidomain equation. To this purpose, we extrapolate the unknown  $V_m$ . More precisely,  $w^{n+1}$  is obtained by  $w^{n+1} = \sum_{j=0}^p a_{j,p} w^{n-j} - \Delta t b_{-1,p} g(\widetilde{V}_m^{n+1}, w^{n+1})$ , where  $\widetilde{V}_m^{n+1} = \sum_{j=0}^q \alpha_{j,q} V_m^{n-j}$  is the extrapolation of order  $q$  of the previously computed  $V_m$ ,  $q$  being the order in time of the scheme used to compute  $V_m$  (see below), and  $\alpha_{j,q}$ ,  $a_{j,p}$  and  $b_{-1,p}$  are the constants of the BDF methods [19].

The second step is to solve the bidomain-torso problem. We use a domain decomposition algorithm: assuming that  $u_T^{n+1,k}$  is given, we compute  $V_m^{n+1,k+1}$  and  $u_e^{n+1,k+1}$  solving a Neumann problem in  $\Omega_H$  with a  $q$ -order BDF time scheme: for all  $\phi$  in the basis of the finite element space

$$\begin{cases} A_m \int_{\Omega_H} C_m V_m^{n+1,k+1} \phi + \Delta t b_{-1,q} \int_{\Omega_H} \sigma_i \nabla(V_m^{n+1,k+1} + u_e^{n+1,k+1}) \cdot \nabla \phi = \\ A_m \int_{\Omega_H} \left( C_m \sum_{j=0}^q \alpha_{j,q} V_m^{n-j} + \Delta t b_{-1,q} I_{\text{ion}}(\widetilde{V}_m^{n+1}, w^{n+1}) \right) \phi + \Delta t b_{-1,q} \int_{\Omega_H} I_{\text{app}} \phi, \\ \int_{\Omega_H} (\sigma_i + \sigma_e) \nabla u_e^{n+1,k+1} \cdot \nabla \phi \\ + \int_{\Omega_H} \sigma_i \nabla V_m^{n+1,k+1} \cdot \nabla \phi = \int_{\Gamma_{\text{epi}}} \sigma_T \nabla u_T^{n+1,k} \cdot \mathbf{n}_T \phi. \end{cases} \quad (3.13)$$

<sup>1</sup> Sundials library, <http://www.llnl.gov/casc/sundials/>

Next, the potential  $u_e^{n+1,k+1}$  being known, we compute  $u_T^{n+1}$  solving the following problem in the torso  $\Omega_T$ :

$$\begin{aligned} & b_{-1,q} \int_{\Omega_T} \boldsymbol{\sigma}_T^{n+1} \nabla u_T^{n+1,k+1} \cdot \nabla \phi + \int_{\Gamma_{\text{epi}}} \left( \frac{b_{-1,q}}{R_p} + \frac{C_p}{\Delta t} \right) u_T^{n+1,k+1} \phi \\ &= \int_{\Gamma_{\text{epi}}} \left( \frac{b_{-1,q}}{R_p} + \frac{C_p}{\Delta t} \right) u_e^{n+1,k+1} \phi + \frac{C_p}{\Delta t} \int_{\Gamma_{\text{epi}}} \sum_{j=0}^q a_{j,q} (u_T^{n-j} - u_e^{n-j}) \phi. \end{aligned} \quad (3.14)$$

To enforce a “strong coupling” (namely the transmission conditions (2.10)), we have to iterate in  $k$  between (3.13) and (3.14) until convergence, at each time step. We can also perform a “weak coupling” by performing only one iteration in  $k$ , or even by replacing condition (2.9)<sub>2</sub> by  $\boldsymbol{\sigma}_e \nabla u_e \cdot \mathbf{n} = 0$ . This approximation will be considered in § 4.2.

## 4 Numerical Results

The torso geometry includes the lungs and the skeleton<sup>2</sup> (see Fig. 1). The heart geometry is simplified – based on intersecting ellipsoids – so that the fibers orientation can be given in terms of analytical functions (see Fig. 1). We refer to [22] for the details of the geometrical definition of the heart. Note that this simplified geometry only includes the ventricles. We therefore cannot simulate P-waves. The finite element meshes of the heart (61 512 tetrahedra) and the torso (311 117 tetrahedra) have been realized with YAMS [8] and GHS3D[9,10].

The conductivity tensors  $\boldsymbol{\sigma}_i$  and  $\boldsymbol{\sigma}_e$  are given by  $\boldsymbol{\sigma}_{i,e}(x) = \sigma_{i,e}^t I + (\sigma_{i,e}^l - \sigma_{i,e}^t) \mathbf{a}(x) \otimes \mathbf{a}(x)$ , where  $\mathbf{a}(x)$  is a unit vector parallel to the local fiber direction (Fig. 1, Left) and  $\sigma_{i,e}^l$  and  $\sigma_{i,e}^t$  are respectively the conductivity coefficients in the intra- and extra-cellular media measured along the fibers direction and in the transverse direction. Experiments show that  $\sigma_{i,e}^l$  and  $\sigma_{i,e}^t$  have different values, which means that intra- and extra-cellular media are anisotropic. We have taken into account this anisotropy. It is also established that they are spatially dependent. In particular, the conductivity is larger in the His bundle and the Purkinje fibers. Nevertheless, this space dependence is not considered in our simulations. The fact that the Purkinje fibers conducts very quickly the electrical signal is roughly modeled by taking an uniform initial stimulation on the endocardium. All the numerical experiments have been obtained with a very small value of  $R_p$ . This amounts to considering the standard transmission conditions (2.9). In the following section, the ECG are plotted according to the standard 12-leads ECG definition (see [14], for instance): DI =  $u_T(L) - u_T(R)$ , DII =  $u_T(F) - u_T(R)$ , DIII =  $u_T(F) - u_T(L)$ , aVR =  $\frac{3}{2}(u_T(R) - u_W)$ , aVL =  $\frac{3}{2}(u_T(L) - u_W)$ , aVF =  $\frac{3}{2}(u_T(F) - u_W)$ ,  $V_i = u_T(V_i) - u_W$ , for  $i = 1, \dots, 6$ , where the points  $L, R, F, (V_i)_{i=1..6}$  are indicated in Fig. 1, and where  $u_W = (u_T(L) + u_T(R) + u_T(F))/3$ .

<sup>2</sup> This geometry comes from Zygote Media Group, Inc. <http://www.zygote.com/>

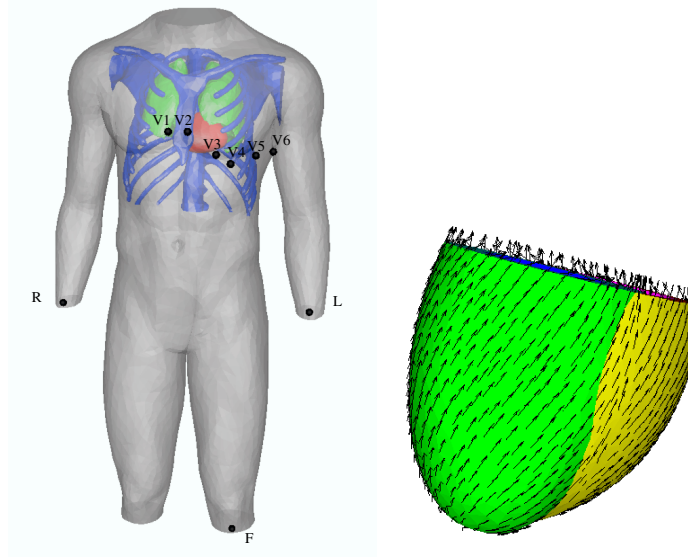


**Fig. 1.** Computational domains: torso and ECG leads (Left), heart with fibers (Right)

#### 4.1 A Reference Simulation

We start from a “reference simulation”, in which we take into account the anisotropy ( $\sigma_{i,e}^l \neq \sigma_{i,e}^t$ ) and a cells heterogeneity across the wall of the left ventricule (see [21] for instance). This heterogeneity is achieved by taking a coefficient  $\tau_{close}$  in (2.6) varying across the thickness direction. The initial stimulation is given by a volume current which acts on the whole endocardium (both left and right parts). The simulated ECG is reported in Fig. 2. Compared to a real ECG, we can notice that the waves have a correct orientation in each of the 12 leads. Some points have still to be improved, in particular the amplitude of the T-wave and the length of the QRS-complex. In the sequel, we play with various modelling assumptions and compare the results with this solution.

#### 4.2 Weak Coupling with Torso

In order to reduce the computational cost of the heart-torso coupling, we can relax the coupling condition (2.9) to

$$u_e = u_T, \quad \text{and} \quad \sigma_e \nabla u_e \cdot \mathbf{n} = 0, \quad \text{on} \quad \Gamma_{\text{epi}}. \quad (4.15)$$

The resulting system (2.7) and (4.15)<sub>2</sub> can be solved independently of the torso. Then, the ECG signals can be recovered in a second step by solving (2.8) with (4.15)<sub>1</sub>. The results are reported in Fig. 3 (for the sake of conciseness we only report the DI, aVr, V1 and V4 leads). A comparison with Fig. 2 shows that the amplitude of the waves is slightly larger with the weak coupling. Nevertheless, the solutions are qualitatively similar. The following experiments will be done with (4.15).

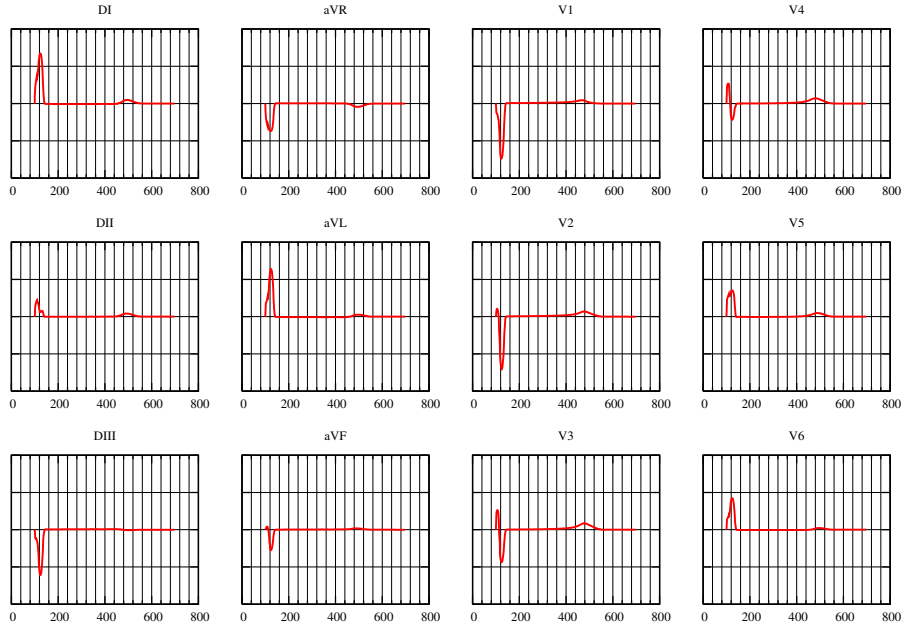


**Fig. 2.** Reference simulation: 12-leads ECG signals obtained by a strong coupling with the torso, including anisotropy and APD inhomogeneity. The units on the  $x$ -axis is milliseconds. The normalization on the  $y$ -axis is arbitrary, but the same on all the results of this paper.

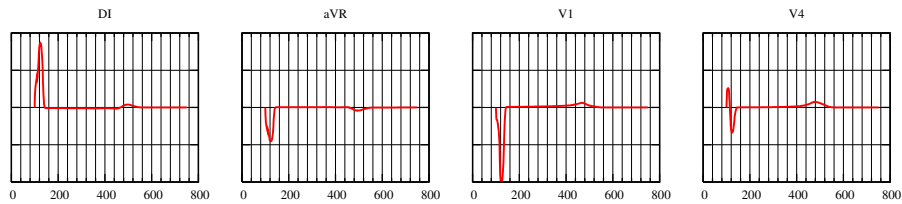


**Fig. 3.** Results obtained with a weak coupling with the torso (compare with Fig. 2)

### 4.3 Impact of Fibers

We now investigate the influence of the anisotropy of the conductivity tensors  $\sigma_i, \sigma_e$  on the ECG signals.

We consider the numerical experiment described in §4.1 but now we consider isotropic conductivities by setting  $\sigma_e^l = \sigma_e^t, \sigma_i^l = \sigma_i^t$ . Fig. 4 shows the corresponding ECG signals. We observe that the QRS-complex has a larger duration than in the anisotropic case (Fig. 2, Top). In addition, the T-wave is inverted in the the first Einthoven limb lead. The influence of anisotropy is much more

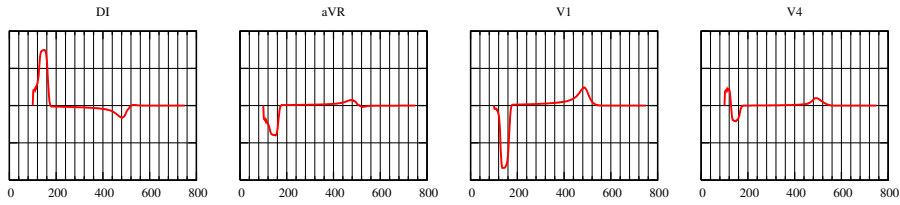


**Fig. 4.** ECG signals: isotropic conductivities

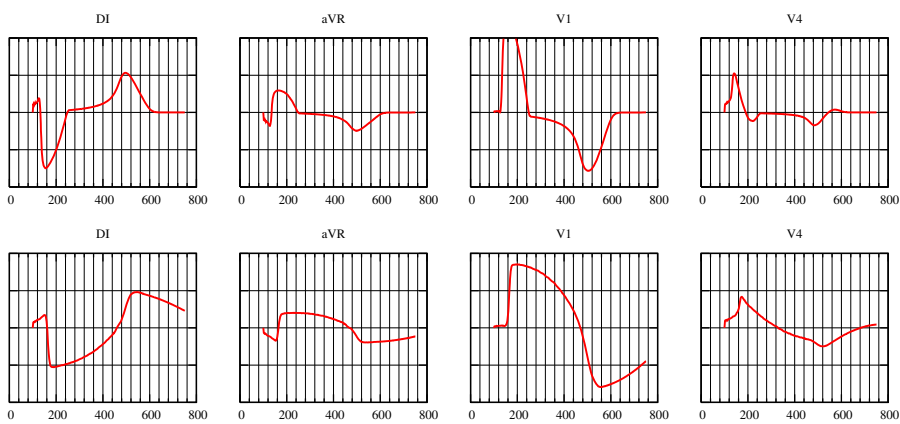


**Fig. 5.** Anisotropic (top) and isotropic (bottom) conductivities in a “pathological” case (right bundle-branch block). The sensitivity to the anisotropy is striking.

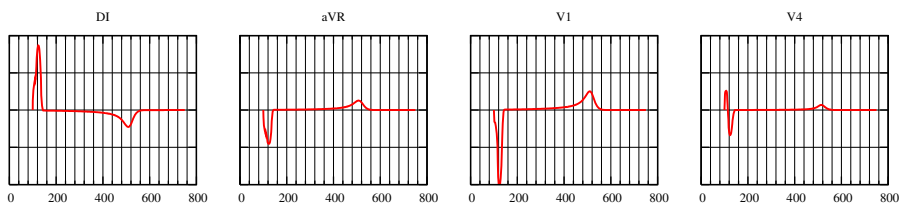


**Fig. 6.** ECG signals: with an homogeneous action potential duration the T-wave has the wrong sign on the first lead (compare with Figure 2)

striking when dealing with pathological stimulations. For instance, in Fig. 5 we have reported, the simulated ECG signals for a pathological stimulation (a right bundle-branch block) with anisotropic (top) and isotropic (bottom) conductivities. As expected, both results show a longer QRS complex compared to Fig. 2.



#### 4.4 Impact of Cell Heterogeneity

We now investigate the role of the action potential duration (APD) heterogeneity on the ECG signals. For the sake of simplicity we restrict ourselves to a transmural heterogeneity, playing with the  $\tau_{close}$  coefficient as mentioned in § 4.1.

In Fig. 6 we have depicted the ECG signals corresponding to an homogeneous APD ( $\tau_{close}$  constant in (2.6)). In the first lead (Fig. 6, Left), we observe that the T-wave is inverted compared to the reference case (Fig. 2, Left-Top) and to what is usually observed in real ECGs.

## 5 Conclusion

We have presented a mathematical model for the electrical activity of the heart coupled to the torso. We started from a reference numerical simulation based on the Mitchell-Schaeffer dynamics, where we took into account the heart-torso coupling, the anisotropy due to the fibers, a simple heterogeneity along the left ventricle wall thickness. The resulting ECG is acceptable on the 12 standard leads. Then, we have shown that cell homogeneity yields inverted T-wave. We have also shown that a strong coupling with the torso has only a small influence on the ECG whereas anisotropy due to fibers orientation has to be taken into account in general. Further computations have to be carried out to confirm these results and to assess other points, like for example the relevance of the transmission conditions (2.10).

**Acknowledgment.** This work was partially supported by the CardioSense3D<sup>3</sup> project (INRIA). We would like to thank Michel Sorine for many fruitful discussions, in particular regarding the heart-torso transmission conditions. We also thank Elsie Phé for her work on the geometries and on the meshes generation.

## References

1. Boulakia, M., Fernández, M.A., Gerbeau, J.-F., Zenzemi, N.: Mathematical analysis of a coupled bidomain-torso model in electrophysiology. Submitted
2. Colli Franzone, P., Pavarino, L.F.: A parallel solver for reaction-diffusion systems in computational electrocardiology. *Math. Models Methods Appl. Sci.* 6(14), 883–911 (2004)
3. Colli Franzone, P., Pavarino, L.F., Taccardi, B.: Simulating patterns of excitation, repolarization and action potential duration with cardiac bidomain and monodomain models. *Math. Biosci.* 1(197), 35–66 (2005)
4. Colli Franzone, P., Savaré, G.: Degenerate evolution systems modeling the cardiac electric field at micro- and macroscopic level. *evolution equations, semigroups and functional analysis. Progr. Nonlin. Diff. Eq. Appl.* 1(50), 49–78 (2002)
5. Coudière, Y., Pierre, C., Turpault, R.: Solving the fully coupled heart and torso problems of electrocardiology with a 3d discrete duality finite volume method. submitted (2006)

<sup>3</sup> <http://www.inria.fr/CardioSense3D>

6. Djabella, K., Sorine, M.: Differential model of the excitation-contraction coupling in a cardiac cell for multicycle simulations. In: EMBEC'05, vol. 11, pp. 4185–4190, Prague (2005)
7. Fitzhugh, R.: Impulses and physiological states in theoretical models of nerve membrane. *Biophys. J.* (1), 445–465 (1961)
8. Frey, P.: Yams: A fully automatic adaptive isotropic surface remeshing procedure. Technical report 0252, Inria, Rocquencourt, France (November 2001)
9. George, P.L.: Improvement on delaunay based 3d automatic mesh generator. *Finite Elements in Analysis and Design* 25(3-4), 297–317 (1997)
10. George, P.L., Borouchaki, H.: ultimate robustness in meshing an arbitrary polyhedron. *Int. J. Numer. Meth. Engng.* 58(7), 1061–1089 (2002)
11. Krassowska, W., Neu, J.C.: Effective boundary conditions for syncytial tissues. *IEEE Trans. Biomed. Eng.* 2(41), 137–199 (1994)
12. Lines, G.: Simulating the electrical activity in the heart. PhD thesis, Department of Informatics, University of Oslo (1999)
13. Luo, C.H., Rudy, Y.: A model of the ventricular cardiac action potential. depolarisation, repolarisation, and their interaction. *Cir. Res.* (68),1071–1096 (1994)
14. Malmivuo, J., Plonsey, R.: Bioelectromagnetism. principles and applications of bioelectric and biomagnetic fields. Oxford University Press, New York (1995)
15. Mitchell, C.C., Schaeffer, D.G.: A two-current model for the dynamics of cardiac membrane. *Bulletin Math. Bio.* (65),767–793 (2003)
16. Neu, J.C., Krassowska, W.: Homogenization of syncytial tissues. *Crit. Rev. Biomed. Eng.* 21(2), 137–199 (1993)
17. Page, E.: Cat heart muscle in vitro. part iii. the extracellular space. *J. Gen. Physiol.* 1(46), 201–213 (1962)
18. Pierre, C.: Modélisation et simulation de l'activité électrique du cœur dans le thorax, analyse numérique et méthodes de volumes finis. PhD thesis, Laboratoire J. Leray, Université de Nantes (2005)
19. Quarteroni, A., Sacco, R., Saleri, F.: Numerical mathematics. In: Texts in Applied Mathematics, 2nd edn. vol. 37, Springer, Heidelberg (2007)
20. Sachse, F.B.: Computational Cardiology: Modeling of Anatomy, Electrophysiology, and Mechanics. Springer, Heidelberg (2004)
21. Sampson, K.J., Henriquez, C.S.: Electrotonic influences on action potential duration dispersion in small hearts: a simulation study. *Am. J. Physiol. Heart Circ. Physiol.* 289, 350–360 (2005)
22. Sermesant, M., Moireau, P., Camara, O., J., S.-M., Andriantsimiavona, R., Cimirman, R., Hill, D.L., Chapelle, D., Razavi, R.: Cardiac function estimation from mri using a heart model and data assimilation: advances and difficulties. *Med. Image Anal.* 10(4), 642–656 (2006)
23. Sundnes, J., Lines, G.T., Cai, X., Nielsen, B.F., Mardal, K.-A., Tveito, A.: Computing the electrical activity in the heart. Springer, Heidelberg (2006)
24. van Capelle, F.H., Durrer, D.: Computer simulation of arrhythmias in a network of coupled excitable elements. *Cir. Res.* 47, 453–466 (1980)